DOI: 10.21917/ijct.2021.0359

VISIBLE WINDOW IMAGE RAY TRACING METHOD TO MODEL RADIO WAVE PROPAGATION IN FEMTOCELLULAR WIRELESS COMMUNICATION

Fathi Awafie[1], Nabeil A. Abujnah[2], Ali Ukasha[3], Ahmed B. Abdurrhman[4], and Ali Alshanokie[5]
[1,3,4,5]Department of Electrical and Electronic Engineering, University of Sabha, Libya
[2]Department of Electrical and Electronic Engineering, Faculty of Engineering, University of Azzaytuna, Libya

Abstract

In this paper, we present the simulation of the characteristics of radio wave propagation in femto-cellular wireless communication environment. The first aim has been to find a correct description of the environment for received wave. The result of the first investigations is that the environment of the indoor wave significantly changes as we change the electric parameters of material constructions. A modified 3D ray tracing image method tool has been utilized which called Visible Window Image Method (VWIM) for the coverage prediction. A detailed analysis about the behavior of the rays using the electromagnetic wave propagation mechanism classification as Line of sight rays, reflected rays, transmitted rays, and diffracted rays are considered.

Keywords:

Propagation Models, Ray Tracing Technique, Femtocell

1. INTRODUCTION

The ray tracing model can be categorized as deterministic approaches, and are based on geometrical optics, instead of the entire domain field simulation. The method partitions the propagation waves into finite angular components, and these propagation components are traced independently and are applied to each the boundary conditions on material interfaces-reflection, transmission, and diffraction. The solution on every observation point can be finally derived by summing the wave contributions.

These ray-based methods compute the possible rays between the emitter and receivers in complex environments and they need to search the rays to compute transmission, reflections and diffractions.

The deterministic wave propagation models are growing their importance day after day, becoming fundamental for the characterization of indoor propagation. Moreover, high simulation accuracy often requires a huge computation time that sorely tries CPU's strength and speed. In most cases hardware empowering is not enough to reduce computer simulation time, which can vary from minutes to weeks [1]. Hence, they tend still to be very time-consuming if the environment is complex, i.e., if there are a large number of obstacles. Therefore, it is necessary to perform a deep optimization on the algorithm and simplifying assumptions on the propagation models are often unavoidable to increase performances and by this condition the optimization is realized. The visible window image model of ray tracing was performed to analysis and simulated the propagation characteristics of the femtocellular propagation channel environment. The focal point of the model the precision and to reduce the computation time execution of the algorithm. The propagation of waves through such structures is a complex process that cannot be rigorously analyzed within a general-purpose program. Therefore, simple models of these structures are necessary to calculate transmitted, reflected, and diffracted fields by means of closed form expressions. By using ray-tracing technique, the ray interactions with the propagation environment are tracked for horizontal polarization and vertical polarization by taking into account the electromagnetic properties of construction materials [2]-[4]. Usually, the accuracy of ray-based methods is limited by the number of rays that can be computed within a reasonable time.

2. RELATED WORK

Classical ray tracing method [7] [14] were the algorithm starts by constructing an image or a projection of the transmitter in all the building surfaces visible to the transmitter. Then the secondary images of the different primary images are constructed on all the surfaces visible to the primary images. It is increasing the time computation, and this is clearly appeared at the model, were presented in [10], which using the 3D algorithm, were includes all possible specular reflections from the wall and ground reflections only

and corner diffractions in the streets. This model used, ε_r=15 and σ=7, and up to 26 wall reflection points and 1 ground reflection are assumed for 3D model. In the model, as in [12], were 3D image method is proposed, and used "approximated illumination area algorithm", with considered 2 reflections and one diffraction edge.

There is evaluation area with a refection objects are considered, and the evaluation area is filled with evaluation points which are equally spaced each other and they have same height. A ray reflected by the object may launch at a point in one of the evaluation points, also rays are launched at evaluation points within an "illuminated area" on the evaluation plane. The model algorithm [12] is developed by [13], where also 3D ray tracing model is proposed (image method) but here the diffracted from edges are included, the model divides illumination area into sectors, where constructing ray paths and checking their validity, the process can be decomposed into a horizontal and vertical sweep. In the case of an image sector, the algorithm [13] define the angles by considering the first grid point in the sector, ray tracing back to the transmitter, recording the wall top and bottom edge elevation angles with respect to the image. For calculation the field strengths, it begins at the transmitter, so the computing the field at all observation points in the coverage area. Since the coverage area is defined to be a rectangular grid, it follows that the perimeter is automatically discretized according to the grid step size of this grid. The algorithm, presented in [13] shows the accuracy and save more computation time, but the total computation time is proportional to the total number of grid points, and this can be expensive for a dense grid over a large area, and this indicted were the computation time for calculation was approximately 32 min. The SBR/Image method [9] [10] is the

algorithm, which finds equivalent sources (images) for each lunched triangular ray tube. Where the triangular ray tubes are shot from Tx in the way to the Rx, and trace each ray tube, which bounces in the plan, and this method, used the theory of geodesic domes [7]. The SBR/Image model seems to be less rigorous than models based on classical image model, and accuracy depends on the radius of the reception sphere. In the beam tracing algorithm [8] [11], replaces the ray with beams that are represented as cones with polygonal cross sections. The beam consists of a collection of rays originating from a transmitter (or an image of the transmitter) and reflected or transmitted from a planar polygon. The Beam tracing algorithm assumes that all the surfaces in the environment are represented as planar polygons. The beams are tested for intersection with the various surface elements in the environment. The polygons that represent the environment are first sorted according to the distance from the beam. The beam intersection tests are carried out with the nearest polygon first. An image of the transmitter is first computed by reflecting the transmitter through the plane of the polygon.

3. ALGORITHM METHODOLOGY ANALYSIS

The algorithm starts with input data consist of a description of the environment, were expressed by vectors, the locations of transmitter and receiver, the electromagnetic data, and the number of reflections, diffractions, and transmissions. After the input data is read, the segments are sorted into the tree. This provides an information about the plane, number of edges, low signal power cut off, kind of antenna, and kind of motion of the receiver. One of the most significant characteristics of the model presented here is that each image is associated with a specific illumination zone, i.e., the area for which the image can give a valid path as shown in Fig.1.

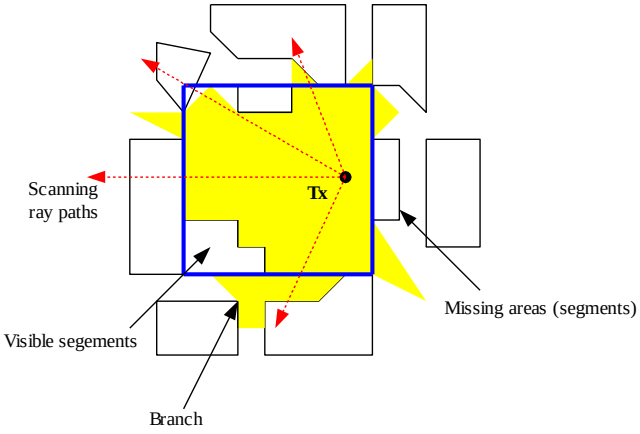

Fig.1. Scanning of visible segments in the illumination area

With this technique, only walls and corners inside the illumination zone of the image can be used for the formation of new images, and moreover, these new images are not valid for the entire wall, but only for the part of the wall illuminated by the parent image.

This new information reduces the number of images and the time for path tracing significantly and makes it feasible for the model to study large complicated environments and trace thousands of rays within seconds. The illumination areas of high-order reflection images tend to become narrower and this prevents the number of images from increasing exponentially with the order of ray interactions with the environment. Hence, the number of images is reduced dramatically since only images which are capable of producing valid paths are generated and stored in the image table. Using illumination area, the time for path tracing is reduced not only because the model has to search for valid paths among fewer images, but also because the images which illuminate a receiver position can now be found very easily with a simple test [5].

The Visible Window Image Ray Tracing Method (VWIM) technique is that instead of scanning and sweep a whole rays, were emitted from *Tx* to the *Rx* at illumination area (visible area), the environment surfaces are divided to the windows, and it is enough to scan fragments (windows), of that visible area to tracing the ray path and check if it's passing through that window, then the image of that path considered be valid and saved in the visible list. Using this definition, the visible window search of image methodology is illustrated and showed in the Fig.2.

With *M* walls, there are *M* images at the 1^{st} level, $(M\text{-}1)M$ images at the 2^{nd} level, $(M\text{-}1)^2 M$ images at the 3^{rd} level, and so forth, and the number of image sources at each level grows rapidly. However, some image sources can be discarded immediately because the walls are not infinite planes. Considering the configuration in Fig.2, where image source *I* is an image in the ceiling *#I*, and at the next level, image source *J* is an image of source *I* in the ground *#J*. The projection of ceiling *#I*, from image source *I* on to ground *#J* is segment *AB* in the plane of ground *#J*, which here the unique reflection is occurred.

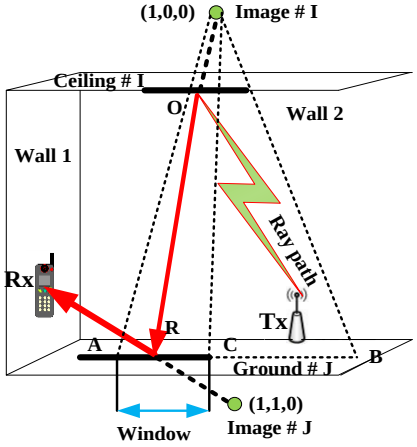

Fig.2. Visible window search of image methodology

The portion of *AB* that lies within the physical area of ground *#J* is segment *AC*, and is called the "window" associated with image source *#J* in ground *#J*. A ray from image source *#J* must pass through the "window" and the unique reflection from the ground is valid. Thus, the ray from *Tx*, reflected at *O* from ceiling *#I*, reflected at *R* from ground *#J*, and reaching the *Rx*, is physically possible. If the segment *AB* on the plane of ground *#J* does not intersect any part of ground *#J*, then the window is of zero extent and image source *J* can be discarded as the image tree is constructed and not saved at the visible list.

This eliminates a great many image sources from the tree. In carrying out ray tracing for the *Rx*, first a ray is traced from image *J* to *Rx*.

The intersection of this ray with the "window" of image source *J*, i.e. line segment *AC*, must lie within the window, or else the ray can be discarded. If the ray is possible, then the ray is traced back to image source *I*, and the intersection of the *IJ* ray with the plane of ceiling *#I* must line within the "window" of image source *I*. If it does then *I* can be joined with the source, *Tx*, and two reflections ray path has been found. In addition, for the diffraction paths only those segment end points (actual edges) contained in the list will be used. For the identification of reflection paths a recursive approach is followed. For all segments visible directly from the *Tx* their mirror image points *Tx′* (virtual sources) with respect to every segment are computed. Then, the visibility list for each *Tx′* is calculated for the sectors defined by *Tx′* and the end points of the visible part of each segment. Also, at every recursion step, all possible diffraction points seen from a virtual source are also identified and stored in a path dictionary. The image source looks out on the world through the window, meaning that rays from the image source must pass through the window to be physically possible.

The concept of "window" eliminates many images from the tree search but is not sufficient as a stopping criterion. The Algorithm uses minimum field strength associated with an image source to terminate the image tree, and choosing specific number of reflections to be used.

4. MATHEMATICAL ANALYSIS

For implementation of the algorithm, the classical formulas for calculating the reflections phenomena, are used for simplicity and avoiding the complexity. When the large number of images involved, we only illustrate one of ray paths with the corresponding images to analysis [6] [15] [16]. The images are labeled (*W*, *G*, *C*), where denote the number of reflections in the walls, in the ground, and ceiling, which indicated in Fig.2. For a ray arriving at *Rx*, all these images from an array, which equivalent sources for the multiple reflections. By using visible window image concept, it enable us to determine the exact point of reflecting at wall or at the ground or ceiling, another advantage of using the visible window image, that from the relative positions of images with respect to the *Rx*, it enable us to identify which if the images will contribute to the received signal and which of the images will not contribute either because of blockage by edges, or because the signal is lost into other environment before reaching *Rx*. So to determine which of the many images will contribute to the total received signal, we tracing the ray path (red path), shown in Fig.2, which contain 2 images. then for illustration purposes the ray path due image (1, 1, 0) , we assuming that we have identified that second image will contribute to the total received signal, and also have determined the number of ground reflection and ceiling reflection, so knowing the image locations alone is not enough to determine the sequence of reflections; it will depend on geometry of the problem [17] [18]. This information is needed to determine the sequence of images for the calculation of reflection points. Assuming in the case that the reflections follow the sequence, as shown in Fig.2, and this sequence represented as $Tx \rightarrow R_C \rightarrow R_G \rightarrow Rx$, then the sequence of images used to calculate the reflection points is given by:

$$Tx \overset{C}{\rightarrow} (1,0,0) \overset{G}{\rightarrow} (1,1,0) \rightarrow Rx \tag{1}$$

Where the first point denotes the reflection from the ceiling, and the second one is reflection from the ground. The reflection points can be then determine as follows: starting from Rx location and the image (1, 1, 0), we calculate the ground reflection point (The last reflection before the signal reaches *Rx*); then from this reflection point and image (1, 0, 0) we calculate the preceding reflection point, where itis the first reflection point. Finally, we need to derive the expression for field contributed by this image (1, 1, 0). Then for the electric vector field for the direct component, LOS case, it depends on the distance between the *Tx* and *Rx*, and for free space loss is given by:

$$\vec{E}_{Dir} = \vec{E}_e \frac{e^{-jk_0 r_d}}{r_d} \tag{2}$$

where

$$\vec{E}_e = \sqrt{\frac{z_0 P_r^{G\vec{E}_0}}{4\pi}} \tag{3}$$

where,

K_0 - free space wave number,

r_d - total path length for the direct ray,

Z_0 - free space impedance,

G - gain of the transmitter antenna,

E_e - emitted electric vector field,

E_0 - source electric vector field of the transmitter antenna and

P_r - power radiated by the transmitter.

For computing the field contribution of the reflected rays we applied the image theory and the reflection coefficients instead of the general expressions of geometrical optics (GO). Taking into account, the reflected field and its components vertical and horizontal.

The general reflected filed can be expressed as:

$$\vec{E}_{\text{Ref}} = \vec{E}_0 \cdot \bar{R} \frac{e^{-jk_0 r_r}}{r_r} \tag{4}$$

where

r_r - total path length for the reflected ray;

$\bar{R}$ - dyadic reflection coefficients $\left(\bar{R} = \prod_{i=1.....n} \bar{R}_i \right)$, and n means the number of reflections for that ray.

For the reflection case, the relative position of the *Tx* with respect to R_C and R_G, the vector electric field at R_G is given by:

$$\vec{E}(R_G) = \vec{E}(R_C) \cdot \bar{R}_1 \cdot \frac{e^{-jk_0 r_{r_1}}}{r_{r_1}} = \vec{E}(R_C) \cdot \bar{R}_{P_1} \tag{5}$$

$$\bar{R}_{P_1} = \bar{R}_1 \cdot \frac{e^{-jk_0 r_{r_1}}}{r_{r_1}} \tag{6}$$

where

$\vec{E}(R_C)$ - incident field at R_C due to *Tx*,

r_{r1} - distance from R_C to *Tx*; and

$\bar{R}_1$ - dyadic reflection coefficient at R_C.

Then the vector electric field at receiver $\vec{E}(R_x)$ due to this ray path can be obtained as follows:

$$\vec{E}(R_x) = \vec{E}(R_G) \cdot \bar{R}_{P_1} = \vec{E}(R_C) \cdot \bar{R}_{P_1} \cdot \bar{R}_{P_2} \quad (7)$$

The total received vector electric field at the receiver antenna is obtained by adding the contribution of each individual rays as follow:

$$\vec{E}_{tot} = \sum_{j=1}^{m} \vec{E}_j \quad (8)$$

where $\vec{E}_j$ is the electric field of the j^{th} ray and it can be $\vec{E}_{Dir}$, $\vec{E}_{Ref}$ and m is the total number of rays reaching the receiver. Then the received power can be written as:

$$P_r = P_t \left(\frac{\lambda}{4\pi} \right)^2 \left| \frac{\vec{E}_{tot}}{\vec{E}_0} \right|^2 \quad (9)$$

5. SIMULATION RESULTS

The algorithm is implemented on a Window 8, and using MATLAB code for analysis and tracing the LOS ray, or the LOS and all the rays that reach the receiver after one reflection or and two-reflection rays etc.

The model was applied to the big hall in electric and electronic department, Sebha University, which has dimension (6m wide, 10m length, and 3m height), as indicated in Fig.3. The simulation was performed for frequency of 3.5GHz, the walls of room are made of concrete, which has dielectric constant (ε =7+j0.4), and there is one door, one made of wood, which has dielectric constant (ε = 2.5+j0.03). The Height of the Tx and Rx antennas are = 1.3m, taken into consideration the height of ceiling from the floor, which equal 3mthe power of Tx = -15dB,

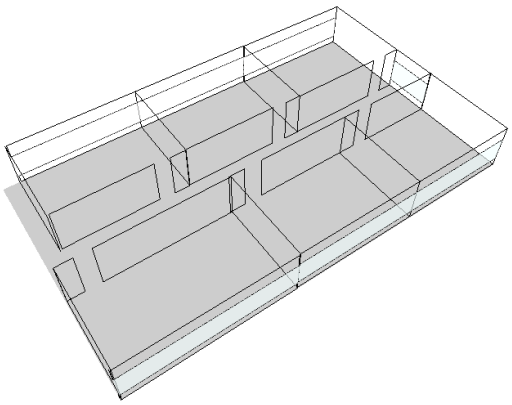

Fig.3. Schematic of the room were the predicted results

From the Figures, one may notice that changes in the antenna height did not have significant effects on the radio wave propagation characteristics in femtocellular environment when compared to the outdoor environments. For that reason, we considered in our work the height of both Tx and Rx antennas are equal, 1.3m.

Received power coverage is investigated for different scenarios. So, the slight difference between the figure results are recognized, the strongest contribution is found near the Tx, where the power was -79dB in Fig.4, for the case of LOS scenario, and when the one reflection adding to the LOS, the result indicated at Fig.5. Where power was between -79.1dB to -123.7dB, but for using only one reflection scenario the power was between -92.3dB to - 128dB and that clearly illustrated in Fig.6.

In Fig.7. the lost more power are clearly appeared when the number of reflections increased to 2, compared with Fig.6. From Fig.6, It is observed that the strongest receiver power levels are in the range of −92.3 to −99.4dB, while strongest receiver power levels are in the range of −101.7 to −107.2dB indicated in Fig.7 the reason for this due to the effect of the phenomenon of reflection on the propagation of the wave where increased the number of reflections from wall.

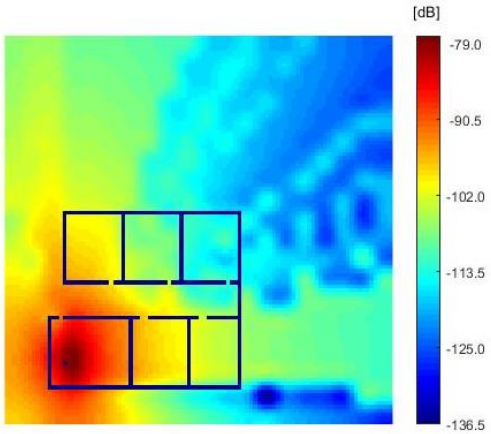

Fig.4. Received power coverage LOS scenario at 3.5GHz

The results show us the most optimistic predictions are distributed within a short distance range from the emitter and receivers. The pessimistic prediction points are located far from the emitter. This may be used as important evidence to further optimize the model. From the simulation results which obtained by using VWIM, it can be concluded that the role of the ray reflections is significant and influencing on the propagation of waves within inside environments

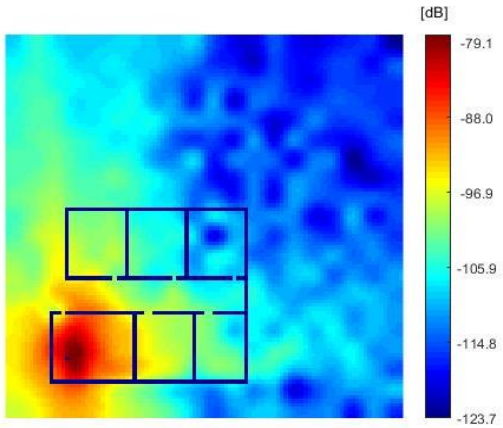

Fig.5. Received power coverage LOS with one reflection scenario at 3.5GHz

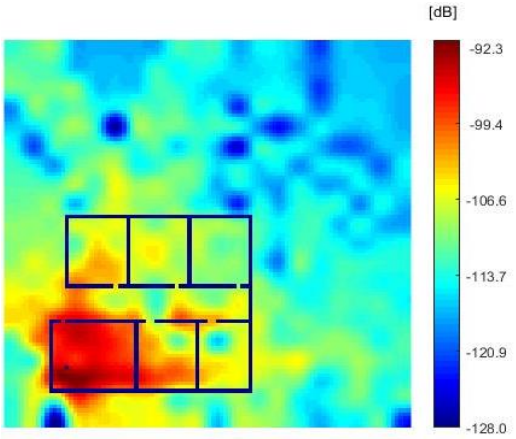

Fig.6. Received power coverage one reflection scenario at 3.5GHz

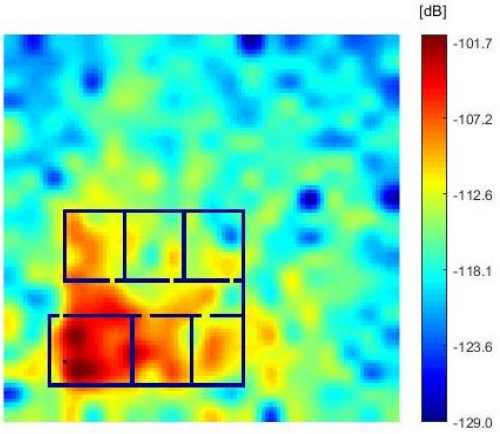

Fig.7. Received power coverage two reflections scenario at 3.5GHz

6. CONCLUSION

The ray tracing technique has been applied to evaluate the received power coverage in small femtocellular room at 3.5GHz for the LOS and reflections ray scenarios. Work reported in this paper has shown that can vary considerably according to the construction of the environment.

By observation of the figures, it can be explained by the fact that the femtocellular environments was complex, and any small variation in the scenarios, data constructions, or position of the receiving antenna led to a substantial variation of the paths between transmitter and receiver, and consequently a noticeable change in the characteristic of propagation channel.

The simulation algorithm has shown that the ray tracing method is a good tool for analysis of radiowave propagation in femtocellular wireless communication characteristics within indoor environment, when multiple reflection mechanism is dominant. Better predictions are possible inside buildings where features and transmission conditions are well known, because, in that case, particular models can be applied.

REFERENCES

[1] M. Allegretti, L. Coppo, R. Notarpietro and G. Perona, "An Enhanced 3D Ray Tracing Algorithm for Indoor EM Propagation", *Proceedings of International Conference on Electromagnetism*, pp. 18-21, 2006.

[2] G. Wolfle, R. Wahl and P. Wertz, "Dominant Path Prediction Model for Indoor Scenarios", *Proceedings of International Conference on Microwave*, pp. 176-179, 2005.

[3] G. Wolfle, B. Gschwendtner and F. Landstorfer, "Intelligent Ray Tracing - A New Approach for the Field Strength Prediction in Microcells", *Proceedings of International Conference on Vehicular Technology*, pp. 790-794, 1997.

[4] G. Wolfle, B. Gschwendtner and F. Landstorfer, "Tracing vs. Ray Launching in 3-D Microcell Modelling", *Proceedings of International Conference on Personal and Mobile Communications*, pp. 74-79, 1995.

[5] F. Alwafie, "Visible Window Image Model of Ray Tracing Technique for Radio Wave Propagation", *Proceedings of International Conference on Microwave and Radar*, pp. 19-23, 2008.

[6] Satvir Singh Sidhu, Arun Khosla and Ashita Sharma, "Implementation of 3-D Ray Tracing Propagation Model for Indoor Wireless Communication", *International Journal of Electronics Engineering*, Vol. 4, No. 1, pp. 43-47, 2012.

[7] M.J. Wenninger, "*Spherical Models*", Cambridge University Press, 1979.

[8] Paul. S. Heckbert and Pat. Hanrahan, "Beam Tracing Polygonal Objects", *Proceedings of International Conference on Computer Graphics and Interactive Techniques*, pp. 119-127, 1984.

[9] S.H. Chen and S.K. Jeng, "An SBR/Image Approach for Radio Wave Propagation in Indoor Environments with Metallic Furniture", *IEEE Transactions Antennas and Propagation*, Vol. 45, No. 1, pp. 98-106, 1997.

[10] S.H. Chen, and S.-K. Jeng, "An SBR/Image Approach to Indoor Radio Propagation Modelling", *Proceedings of International Conference on Antennas and Propagation Society*, pp. 1952-1955, 1995.

[11] S. Fortune, "Efficient Algorithms for Prediction of Indoor Radio Propagation", *Proceedings of International Conference on Vehicular Technology*, pp. 572-576, 1998.

[12] T.S. Rappaport, B.D. Woerner and J.H. Reed, "*Wireless Personal Communications: The Evolution of Personal Communication Systems*", Kluwer Academic Publishers, 1996.

[13] W.M. O`Brien, E.M. Kenny and P.J. Cullen, "An Efficient Implementation of a Three Dimensional Microcell Propagation Tool for Indoor and Outdoor Urban Environments",.*IEEE Transactions on Vehicular Technology*, Vol. 49, No. 2, pp. 622-630, 2000.

[14] H. Sang Kim, "Measurement and Model Based Characterization of Indoor Wireless Channels", Ph.D. Dissertation, Department of Computer Science, University of Massachusetts, pp. 1-190, 2003.

[15] O. Fernandez, L. Valle, M. Domingo and R.P. Torres, "Accurate Ray Tracing for Planning and Design of Wireless Systems", *Proceedings of International Conference on Vehicular Technology*, pp. 1-7, 2008.

[16] Z. Yun and M. F. Iskander, "Ray Tracing for Radio Propagation Modeling: Principles and Applications", *IEEE Access*, Vol. 3, pp. 1089-1100, 2015.

[17] Stevan Grubisic and Walter Pereira Carpes, "An Efficient Indoor Ray-Tracing Propagation Model with A QUASI-3D Approach", *Journal of Microwaves, Optoelectronics and Electromagnetic Applications*, Vol. 13, No. 2, pp. 166-176, 2014.

[18] T.K. Geok, F. Hossain and M.N. Kamaruddin, "A Comprehensive Review of Efficient Ray-Tracing Techniques for Wireless Communication", *International Journal on Communications Antenna and Propagation*, Vol. 8, pp 123-136, 2018.